Original Article | Thyroid

https://doi.org/10.3348/kjr.2018.19.5.992
pISSN 1229-6929 · eISSN 2005-8330
Korean J Radiol 2018;19(5):992-999

Korean Journal of Radiology
KJR

Complementary Role of Elastography Using Carotid Artery Pulsation in the Ultrasonographic Assessment of Thyroid Nodules: A Prospective Study

Soo Yeon Hahn, MD, Jung Hee Shin, MD, Eun Young Ko, MD, Jung Min Bae, MD, Ji Soo Choi, MD, Ko Woon Park, MD

All authors: Department of Radiology and Center for Imaging Science, Thyroid Center, Samsung Medical Center, Sungkyunkwan University School of Medicine, Seoul 06351, Korea

Objective: The aim of this study was to evaluate the diagnostic performance of gray-scale ultrasonography (US), Doppler scan, and elastography using carotid artery pulsation in the diagnosis of thyroid nodules and to find a complementary role of elastography.

Materials and Methods: A total 197 thyroid nodules with 91 malignant and 106 benign pathologic results from 187 patients (41 males and 146 females; age range, 20–83 years; mean age, 49.4 years) were included in this prospective study. The gray-scale, Doppler US images, elastography with elasticity contrast index (ECI), and stiffness color were assessed. The diagnostic performances of each dataset were assessed in order to differentiate benign from malignant thyroid nodules.

Results: The optimal cut-off value of the ECI was 1.71. The area under receiver operating characteristic curve (Az value) was 0.821 for gray-scale US, 0.661 for the ECI, 0.592 for stiffness color, and 0.539 for Doppler US. The Az value for a combined assessment of gray-scale US and the ECI was higher than that for the gray-scale US alone; however, there was no statistical difference between the two (p = 0.219). The median ECI values of follicular thyroid carcinoma (FTC) and follicular variant of papillary thyroid carcinoma (FVPTC) were significantly lower than those of the other malignant lesions (p = 0.005). Meanwhile, the diffuse sclerosing variant of PTC and a metastatic nodule showed the two highest median values of the ECI.

Conclusion: For differentiating thyroid nodules, the diagnostic performances of the combination of gray-scale US and elastography with the ECI were similar to, but not superior, to those of gray-scale US alone. FVPTC and FTC have a significantly lower ECI value than those of the other malignant lesions.

Keywords: *Ultrasonography; Ultrasound; Elastography; Thyroid nodules; Carotid artery pulsation; Elasticity contrast index; Diagnosis; Diagnostic performance*

Received September 14, 2017; accepted after revision March 19, 2018.
This study was supported in part by the research fund of Samsung Medison.

Corresponding author: Jung Hee Shin, MD, Department of Radiology and Center for Imaging Science, Thyroid center, Samsung Medical Center, Sungkyunkwan University School of Medicine, 81 Irwon-ro, Gangnam-gu, Seoul 06351, Korea.
• Tel: (822) 3410-2518 • Fax: (822) 3410-0049
• E-mail: helena35@hanmail.net

INTRODUCTION

Ultrasonography (US) is an accurate modality for noninvasive identification and evaluation of thyroid nodules; however, the sensitivity and specificity of US alone are relatively low, in the ranges of 52–81% and 54–83%, respectively (1). To overcome these limitations, US malignancy risk stratification systems for thyroid nodules and noninvasive additional US techniques for identifying malignancy have been introduced. Ever since Horvath et al. (2) initially introduced the Thyroid Imaging Reporting and Data System (TIRADS), US risk stratification systems for thyroid nodules have been investigated in many

Korean Journal of Radiology
KJR

studies (3-9). Recently, Shin et al. (10) revised the Korean TIRADS (K-TIRADS) with regard to US-based diagnosis and management of thyroid nodules in clinical practices (10).

As a noninvasive additional US technique for thyroid evaluation, several guidelines have considered the color Doppler US feature of central vascularity as a US predictor of malignancy (11, 12) and one of the suspicious US features (9, 13). However, the role of Doppler US examination remains a matter of debate in the literatures (14-17).

Ultrasonography elastography is a relatively new and noninvasive technique developed to obtain information on tissue stiffness (18-21). As described in the literature (22), elastography is used complementary to conventional gray-scale and Doppler US for improving the diagnosis of thyroid nodules, which appear harder than the surrounding tissue. The European Federation of Societies for Ultrasound in Medicine and Biology Guidelines stated that tissue found to be hard on an elastography scan is closely correlated with malignant disease (23). As the US elastography has developed, a new thyroid elastography technique that uses carotid artery pulsation as the internal compression source has recently been introduced as a way of reducing the limitations of elastography, such as variability of the different compression levels by the operators (24) and the out-of-plane motion during external compression (25). Based on this new technique, the elasticity contrast index (ECI) can be obtained through a quantitative scoring method. Lim et al. (26) previously reported good interobserver agreement and intraobserver reproducibility with this technique. In addition, Cho et al. (27) recently demonstrated the diagnostic efficacy of the ECI value for thyroid nodules with US-pathology discordance. In this prospective study, we evaluated the diagnostic performance of gray-scale US and Doppler US based on the K-TIRADS and elastography, using carotid artery pulsation in the differential diagnosis of thyroid nodules, and we tried to find a complementary role for elastography.

MATERIALS AND METHODS

This prospective study was approved by the ethics committee at our institution, and all patients provided written informed consent.

Patients

Between November 2015 and February 2016, 241 consecutive patients, who had 253 thyroid nodules, were included in this study. All of the nodules were ≥ 1 cm in diameter, and the patients were scheduled for biopsy or surgery at the time of US examination. Of these patients, 54 were excluded because the cytohistologic diagnosis was incomplete (n = 14), some nodules were not followed up by US assessment (n = 36), or there was incomplete data acquisition at elastography (n = 4). Finally, a total 197 thyroid nodules with 91 malignant and 106 benign pathologic results from 187 patients (41 male and 146 female; age range, 20–83 years; mean age, 49.4 years) were included in this prospective study.

Real-Time US, Doppler US, and Elastography

Before starting this prospective study, a consensus meeting was held to establish a consensus in the study protocols and the lexicon for the US criteria. During a consensus meeting, three experienced radiologists evaluated images and assessed the lexicon for the US criteria of 30 biopsy-proven thyroid nodules not included in this study. In addition, before starting the study, all three radiologists employed the thyroid elastography technique in the assessment of more than 30 nodules.

Conventional gray-scale US, Doppler US, and elastography were performed using a US system (RS80A with Prestige, Samsung Medison, Co. LTD., Seoul, Korea) with dedicated elastography quantitative software (Samsung Medison, Co. LTD.) with a 5–13 MHz linear transducer. One of three board-certified radiologists with more than 8 years of experience specializing in thyroid imaging performed all the imaging examinations. The gray-scale US images were prospectively evaluated and categorized according to the K-TIRADS by the same radiologist who performed the US examinations. The final K-TIRADS category was decided as high suspicion, intermediate suspicion, low suspicion, or benign nodule based on the malignancy risk stratified by US patterns composed of integrated solidity, echogenicity, presence of microcalcification, orientation, and margin (10). Category 1 represented no nodule; category 2, a benign nodule (spongiform, pure cyst, or partially cystic nodule with comet tail artifact, < 3% malignancy risk); category 3, low suspicion nodule (partially cystic or isohyperechoic nodule without any of the three suspicious US features, 3–15% malignancy risk); category 4, intermediate suspicion nodule (solid hypoechoic nodule without any of the three suspicious US features or partially cystic or isohyperechoic nodule with any of the three suspicious US features, 15–50% malignancy risk); and category 5, high suspicion

nodule (solid hypoechoic nodule with any of the three suspicious US features, > 60% malignancy risk).

Doppler US was performed to assess vascularity during the same US examination by the same operator. The vascularity patterns of the thyroid nodules were categorized as four types, according to the K-TIRADS: type 1, absence of nodule vascularity; type 2, perinodular vascularity only; type 3, mild intranodular vascularity with or without perinodular vascularity (vascularity < 50%); and type 4, marked intranodular vascularity with or without perinodular vascularity (vascularity > 50%). Elastography was also performed by the same radiologist who performed the gray-scale and Doppler US. No external compression with the transducer was applied because carotid artery pulsation was used as the compression source. As a consequence, the nodules were colored depending on their stiffness. On the upper right side of the screen, a scale indicates stiff and soft areas with red and blue colors, respectively (Fig. 1). The operator decided on the predominant color of the thyroid nodules and recorded it. The elasticity parameter, ECI, was determined by manually setting the region of interest within the lesion; once the region of interest was manually set, the ECI was automatically calculated and recorded. To minimize possible observer variability or effects of environmental factors, the operator measured the ECI values once from the transverse plane and once from the longitudinal plane. The ECI values were measured once at each plane.

Data and Statistical Analysis

Thyroid nodules with malignant pathologic results at surgery (n = 81), with malignant cytologic results being confirmed at least twice (n = 6), or with suspicious malignant cytologic results on initial fine needle aspiration (FNA) and malignant results on follow-up core needle biopsy (CNB) (n = 3) were finally classified as malignant.

Thyroid nodules were finally classified as benign when benign pathologic results were obtained at surgery (n = 34); benign cytologic results were confirmed at least twice (n = 27); benign cytologic results were found on both initial FNA and follow-up CNB (n = 10); and there was no increase in size (n = 27) or decrease in size on follow-up US (n = 8). For the reference standard, all initial and repeat biopsy results were included, regardless of the study period.

All data were collected prospectively and recorded by each radiologist in a computerized spreadsheet (Excel; Microsoft, Redmond, WA, USA). We used the χ^2 test for categorical variables, the *t* test for continuous variables with normal distribution, and the Mann-Whitney U test for continuous variables with non-normal distribution to compare the differences in demographic and US characteristics between patients with benign and malignant thyroid nodules. The malignancy rate in each K-TIRADS category based on the gray-scale US was calculated in terms of percentage of malignancy.

In terms of ECI parameters, positive results for transverse and longitudinal elasticity values were determined using the cut-off values obtained with the Youden index (28), and we decided which ECI value was more accurate. The Kruskal-Wallis nonparametric rank sum test was used to test for equality of population medians among the different types of

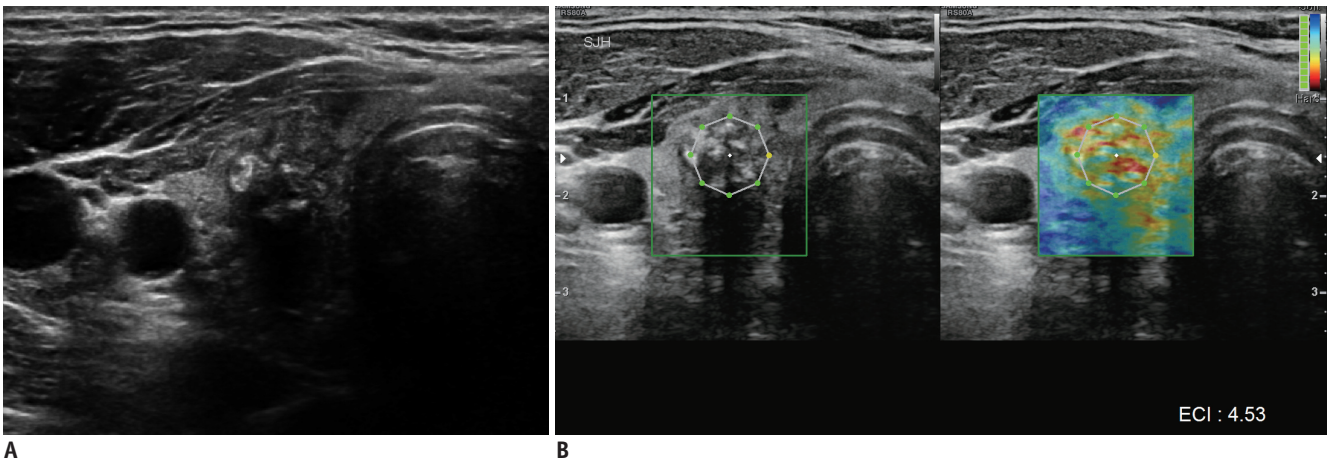

A B

Fig. 1. Gray-scale US (A) and elastography (B) of malignant thyroid nodule. Gray-scale US images **(A)** show solid hypoechoic nodule with spiculated margins and calcifications in right lobe of thyroid gland. This nodule was classified as K-TIRADS category 5. At elastography evaluation **(B)**, this nodule presents stiff pattern (red) in elastography ROI (green box) and high elasticity contrast index (4.53) calculated from ROI (white octagon). This nodule was confirmed as papillary thyroid carcinoma after surgery. ECI = elasticity contrast index, K-TIRADS = Korean Thyroid Imaging Reporting and Data System, ROI = region of interest, US = ultrasonography

Korean Journal of Radiology
KJR

thyroid nodules.

The diagnostic performances of gray-scale US, Doppler US, and elastography for differentiating malignant from benign thyroid nodules were evaluated. The areas under the curve (Az) values were compared by the receiver operating characteristic (ROC) curve analysis with 95% confidence intervals (CIs). The diagnostic performance of the ECI with various cut-off values was evaluated, along with the sensitivity, specificity, positive predictive value (PPV), and negative predictive value (NPV). The diagnostic performances of the K-TIRADS category of gray-scale US, ECI of elastography, and the combined assessment of both techniques using the optimal ECI cut-off value were evaluated and compared using McNemar's test. For the combined assessment of gray-scale US and elastography, the K-TIRADS category was downgraded or upgraded when an ECI value indicated perfect predictive value with no false negatives or false positives.

The statistical analysis was performed using SPSS® version 23.0 software (IBM Corp., Armonk, NY, USA), and statistical significance was accepted as a p value of less than 0.050.

RESULTS

The clinical and imaging characteristics of the 187 patients and the 91 malignant and 106 benign thyroid nodules are summarized in Table 1. The mean age of patients with malignant thyroid nodules was significantly younger than that of those with benign nodules (p = 0.000). The mean size of the malignant thyroid nodules was significantly smaller than that of the benign nodules (p = 0.005). Calcifications were more frequently seen in malignant than in benign nodules (p = 0.000). K-TIRADS categories based on gray-scale US were higher in the malignant group than in the benign group (p = 0.000). The malignancy rate in each K-TIRADS category was 0% (0/18) for category 2, 20.2% (18/89) for category 3, 54.1% (20/37) for category 4, and 100% (53/53) for category 5. The ECI was significantly higher in malignant nodules than in benign thyroid nodules (p < 0.001). Type 4 vascularity

Table 1. Characteristics of Benign and Malignant Thyroid Nodules

	Benign (n = 106)	Malignant (n = 91)	*P*
Age (years)			< 0.001*
Mean ± SD	53.0 ± 10.4	46.0 ± 11.9	
Sex (number of patients)			0.001*
Male	14 (13.2)	31 (34.1)	
Female	92 (86.8)	60 (65.9)	
Gray-scale US			
Size (mean ± SD, cm)	2.5 ± 1.3	2.0 ± 1.1	0.007*
Presence of calcifications			< 0.001*
Yes	23 (21.7)	55 (60.4)	
No	83 (78.3)	36 (39.6)	
K-TIRADS category			< 0.001*
2	18 (17.0)	0 (0.0)	
3	71 (67.0)	18 (19.8)	
4	17 (16.0)	20 (22.0)	
5	0 (0.0)	53 (58.2)	
Elastography			
ECI value (median ± SD)	1.45 ± 0.89	2.06 ± 1.15	< 0.001*
Stiffness color			0.010*
Red	48 (45.3)	58 (63.7)	
Not red	58 (54.7)	33 (36.3)	
Doppler US			0.009*
Type 1 (none)	13 (12.3)	18 (19.8)	
Type 2 (perinodular vascularity)	29 (27.4)	11 (12.1)	
Type 3 (mild intranodular vascularity)	51 (48.1)	40 (44.0)	
Type 4 (marked intranodular vascularity)	13 (12.3)	22 (24.2)	

Data are numbers of lesions. Numbers in parentheses are percentages (%). *p < 0.050 was regarded as statistically significant. ECI = elasticity contrast index, K-TIRADS = Korean Thyroid Imaging Reporting and Data System, SD = standard deviation, US = ultrasonography

(marked intranodular vascularity) on Doppler US and stiffness color (red) on elastography were more frequent in malignant thyroid nodules (p = 0.009 and p = 0.010).

The transverse measurement method was the more accurate elastography technique, achieving an area under the ROC curve of 0.693 (95% CI 0.620–0.766) and having an optimal cut-off value of 1.71. The longitudinal ECI measurement method had an area under the ROC curve of 0.635 (95% CI 0.557–0.714), and its best cut-off value was 1.91. In this study, an ECI value in a transverse measurement was adopted as the appropriate measure for suspected malignancy in the evaluation of thyroid nodules.

Table 2 lists the diagnostic performance of the ECI with various cut-off values for the differential diagnosis of thyroid nodules as benign or malignant. The optimal cut-off value of the ECI was 1.71 with estimated sensitivity 67%, specificity 65.1%, PPV 62.5%, and NPV 69.3%. No benign nodules had ECI values ≥ 4.27, and no malignant nodules had ECI values ≤ 0.67.

The cytopathologic and histopathologic diagnoses and correlation of ECI values are summarized in Table 3. The median ECI value of follicular thyroid carcinoma (FTC) and follicular variant of papillary thyroid carcinoma (FVPTC) was significantly lower than those of the other malignant lesions (p = 0.005). However, there was no significant difference in the ECI among the benign thyroid nodules (p = 0.299). Meanwhile, a diffuse sclerosing variant of PTC and a metastatic nodule showed the two highest median values of the ECI.

The Az values for each dataset were 0.821 (95% CI 0.759–0.883) for K-TIRADS category of gray-scale US, 0.661 (95% CI 0.584–0.737) for ECI of elastography, 0.592 (95% CI 0.513–0.672) for stiffness color of elastography, and 0.539 (95% CI 0.458–0.619) for Doppler US (Fig. 2). Therefore, we applied K-TIRADS and the ECI in order to evaluate and compare the diagnostic performance of the imaging methods.

For the combined assessment of gray-scale US and elastography, the reader downgraded the K-TIRADS category when an ECI ≤ 0.67 was assigned, and upgraded the K-TIRADS category when an ECI of ≥ 4.27 was assigned. For lesions with an ECI between 0.67 and 4.27, the K-TIRADS category was not changed. The Az value for a combined assessment of the gray-scale US and the ECI was higher than that for the gray-scale US alone; however, there was no statistical difference (p = 0.219) (Table 4). Using the combined assessment of both techniques, the sensitivity (80.2%) and specificity (87.7%) were significantly higher than those of elastography with the ECI alone (67.0% and 65.1%) (p = 0.034).

Table 2. Diagnostic Performance of ECI for Various Cut-Off Values in Differential Diagnosis of Thyroid Nodules

ECI Value*	Sensitivity (%)	Specificity (%)	PPV (%)	NPV (%)
0.67	100.0	8.5	48.4	100.0
1.71	67.0	65.1	62.5	69.3
4.27	11.0	100.0	100.0	56.7

*No benign nodules had ECI values ≥ 4.27, no malignant nodules had ECI values ≤ 0.67, and optimal cut-off value of ECI was 1.71. NPV = negative predictive value, PPV = positive predictive value

Table 3. Cytopathologic and Histopathologic Diagnosis and Correlation with ECI in 197 Thyroid Nodules

Diagnosis	ECI		
	Median	Range	SD
Benign thyroid nodules (n = 106)	1.44	0.41–4.26	0.89
Benign follicular nodule (n = 78)	1.47	0.52–4.26	0.91
Chronic lymphocytic thyroiditis (n = 2)	1.85	1.71–1.99	0.14
Nodular hyperplasia (n = 11)	1.15	0.67–4.05	1.07
Follicular adenoma (n = 15)	1.20	0.41–2.13	0.44
Malignant thyroid nodules (n = 91)	2.06	0.68–5.64	1.15
FTC (n = 7)	1.42	0.78–3.94	1.05
Classic PTC (n = 70)	2.19	0.71–5.64	1.17
FVPTC (n = 11)	1.45	0.68–2.39	0.57
Diffuse sclerosing variant of PTC (n = 2)	2.85	2.41–3.28	0.44
Metastasis from lung cancer (n = 1)	2.67	NA	NA

FTC = follicular thyroid carcinoma, FVPTC = follicular variant of papillary thyroid carcinoma, NA = not applicable

Korean Journal of Radiology
KJR

DISCUSSION

Ultrasonography elastography was developed to obtain information on tissue stiffness noninvasively (18-21), and it is used complementary to conventional gray-scale and Doppler US for improving the diagnosis of thyroid nodules, which appear harder than the surrounding tissue (22). In this study, we employed a new elastographic technique that uses carotid artery pulsation as a compression source for thyroid elastography, which was more regular and objective than manual external compression. This technique was first introduced by Bae et al. (24) in a preliminary study indicating the feasibility of pulsation-induced thyroid strain elastography and was later assessed in various studies (24, 26, 27, 29-33).

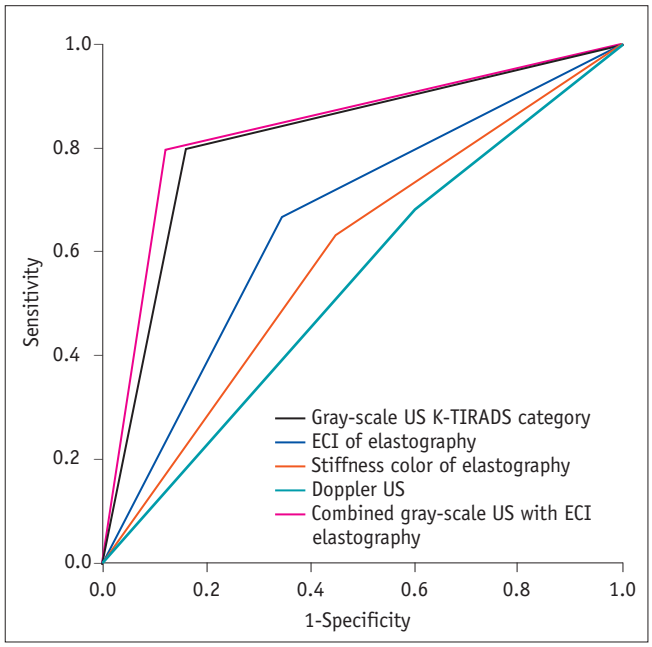

Fig. 2. Receiver operating characteristic curves for gray-scale US K-TIRADS category, ECI and stiffness color of elastography, Doppler US, and combined gray-scale US with ECI elastography for differentiation of benign from malignant thyroid nodules.
Az value was 0.821 (95% CI 0.759–0.883) for K-TIRADS category of gray-scale US, 0.661 (95% CI 0.584–0.737) for ECI of elastography, 0.592 (95% CI 0.513–0.672) for stiffness color of elastography, 0.539 (95% CI 0.458–0.619) for Doppler US, and 0.840 (95% CI 0.780–0.900) for combined gray-scale US with ECI elastography, respectively. Az = area under receiver operating characteristics curve, CI = confidence interval

Previously, several studies have analyzed the efficacy of elastography for differentiating between benign and malignant thyroid nodules. Some of these studies reported that the diagnostic performance of elastography was similar to or higher than that of gray-scale US (31, 33-35). They concluded that the high specificity of elastography could play an adjunctive role in enhancing the diagnostic performance of gray-scale US. In our study, to assess the diagnostic performance of quantitative elastographic parameters, we derived cut-off values of 0.67 and 4.27 for the lower and upper limits of the ECI, respectively. For the combination of gray-scale US and elastography, the ECI with these cut-off values was used, because it resulted in the highest Az value of all the combinations of diagnostic methods, but this finding was not statistically significant. Cho et al. (27) recently evaluated the diagnostic accuracy of the ECI, using a different study design, but they obtained results similar to ours.

For quantification of the local strain contrast within a nodule, the ECI has been used as the parameter for elastography using carotid artery pulsation (24, 26, 27, 29-33). In this study, our cut-off value for the ECI was lower than those in previous studies for differentiating malignant from benign thyroid nodules (27, 31-33). The relatively high cut-off value (ranging from 2.45 to 3.60) of those studies may be a consequence of the small number of

Table 4. Diagnostic Performances of K-TIRADS Category for Gray-Scale US, ECI of Elastography, and Combined Assessment of both Techniques in Differentiation of Thyroid Nodules

	Az (95% CI)	Sensitivity (%)	*P*	Specificity (%)	*P*	Accuracy (%)	*P*	PPV (%)	*P*	NPV (%)	*P*
K-TIRADS category of gray-scale US	0.821 (0.759–0.883)	80.2		84.0		82.2		81.1		83.2	
ECI of elastography	0.661 (0.584–0.737)	67.0	0.052	65.1	0.004	66.0	< 0.001	62.2	0.250	69.7	0.004
Combination of gray-scale US and ECI	0.840 (0.780–0.900)	80.2	1.0* 0.045†	87.7	0.125* < 0.001†	84.3	0.063* < 0.001†	84.9	1.0* 0.500†	83.8	0.125* < 0.001†

K-TIRADS category was downgraded if lesions showed ECI ≤ 0.67 and upgraded if lesions showed ECI ≥ 4.27. *Comparison between gray-scale US and combination of both techniques, †Comparison between elastography and combination of both techniques. Az = area under receiver operating characteristics curve, CI = confidence interval

malignant cases, a comparatively homogeneous population of malignant cases (almost whole numbers of PTC), the malignant cases with small sizes (less than 1 cm), or narrow inclusion criteria (indeterminate US features only). Meanwhile, our study included a larger number of malignant nodules with various types of histology and various US findings, and it excluded nodules less than 1 cm in size. In particular, FVPTC and FTC comprised 19.8% of malignant thyroid nodules (12.1% and 7.7%, respectively). Our median ECI value for total malignant nodules was 2.06 ± 1.15, while those for the FVPTC and FTC were, respectively, 1.45 ± 0.57 and 1.42 ± 1.05, which was much closer to benign (1.45 ± 0.89) than malignant nodules.

In the present study, we applied the K-TIRADS to stratify the malignancy risk of thyroid nodules on gray-scale US. The malignancy rate for each K-TIRADS category was as follows: 0% for category 2, 20.2% for category 3, 54.1% for category 4, and 100% for category 5. Our malignancy rates for categories 3 and 4 were slightly higher than the expected malignancy risk (10). Because our institution is a referral center, the proportion of malignant thyroid nodules in our patient population might be higher than that of other institutions. As described above, 19.8% of our malignant cases were diagnosed as FVPTC or FTC. According to the studies (36-38), FVPTC and FTC have less frequent malignant US findings compared to classic PTC. Therefore, these tumors should be considered when they lack malignant US appearances (category 3 and 4) and have a lower ECI of elastography, but being malignant or follicular neoplasms at cytology.

This study had several limitations. First, interobserver variability was not evaluated in the assessment of US and elastography. Second, patient factors (e.g., weight, pressure, and combinations of diseases such as diabetes mellitus, hypertension, and atherosclerosis) and nodule factors (e.g., distance of the nodule from the carotid artery) that might influence the diagnostic accuracy of US elastography were not analyzed. Because we used carotid artery pulsation as the compression source, these factors could have affected the results of elastography. Kim et al. (39) reported that elastography results for nodules within 1 cm distance of the carotid artery should be interpreted with caution. To reflect daily practice conditions, in this study we evaluated all nodules regardless of location.

In conclusion, for differentiating thyroid nodules, the diagnostic performances of a combination of gray-scale US and elastography with ECI were similar but not superior to those of gray-scale US alone. FVPTC and FTC have a significantly lower ECI value than those of the other malignant lesions.

REFERENCES

1. Fish SA, Langer JE, Mandel SJ. Sonographic imaging of thyroid nodules and cervical lymph nodes. *Endocrinol Metab Clin North Am* 2008;37:401-417, ix
2. Horvath E, Majlis S, Rossi R, Franco C, Niedmann JP, Castro A, et al. An ultrasonogram reporting system for thyroid nodules stratifying cancer risk for clinical management. *J Clin Endocrinol Metab* 2009;94:1748-1751
3. Seo H, Na DG, Kim JH, Kim KW, Yoon JW. Ultrasound-based risk stratification for malignancy in thyroid nodules: a four-Tier Categorization System. *Eur Radiol* 2015;25:2153-2162
4. Park JY, Lee HJ, Jang HW, Kim HK, Yi JH, Lee W, et al. A proposal for a thyroid imaging reporting and data system for ultrasound features of thyroid carcinoma. *Thyroid* 2009;19:1257-1264
5. Kwak JY, Han KH, Yoon JH, Moon HJ, Son EJ, Park SH, et al. Thyroid imaging reporting and data system for US features of nodules: a step in establishing better stratification of cancer risk. *Radiology* 2011;260:892-899
6. Kwak JY, Jung I, Baek JH, Baek SM, Choi N, Choi YJ, et al.; Korean Society of Thyroid Radiology (KSThR); Korean Society of Radiology. Image reporting and characterization system for ultrasound features of thyroid nodules: multicentric Korean retrospective study. *Korean J Radiol* 2013;14:110-117
7. Haugen BR, Alexander EK, Bible KC, Doherty GM, Mandel SJ, Nikiforov YE, et al. 2015 American Thyroid Association management guidelines for adult patients with thyroid nodules and differentiated thyroid cancer: the American Thyroid Association guidelines task force on thyroid nodules and differentiated thyroid cancer. *Thyroid* 2016;26:1-133
8. Park JM, Choi Y, Kwag HJ. Partially cystic thyroid nodules: ultrasound findings of malignancy. *Korean J Radiol* 2012;13:530-535
9. National Comprehensive Cancer Network, Inc. 2014 Practice Guidelines in Oncology—Thyroid Carcinoma v.2. Web site. http://www.nccn.org/professionals/physician_gls/f_guidelines.asp. Accessed April 9, 2018
10. Shin JH, Baek JH, Chung J, Ha EJ, Kim JH, Lee YH, et al.; Korean Society of Thyroid Radiology (KSThR) and Korean Society of Radiology. Ultrasonography diagnosis and imaging-based management of thyroid nodules: revised Korean Society of Thyroid Radiology consensus statement and recommendations. *Korean J Radiol* 2016;17:370-395
11. Papini E, Guglielmi R, Bianchini A, Crescenzi A, Taccogna S, Nardi F, et al. Risk of malignancy in nonpalpable thyroid nodules: predictive value of ultrasound and color-Doppler features. *J Clin Endocrinol Metab* 2002;87:1941-1946
12. Iared W, Shigueoka DC, Cristófoli JC, Andriolo R, Atallah AN, Ajzen SA, et al. Use of color Doppler ultrasonography for

the prediction of malignancy in follicular thyroid neoplasms: systematic review and meta-analysis. *J Ultrasound Med* 2010;29:419-425
13. Gharib H, Papini E, Paschke R, Duick DS, Valcavi R, Hegedüs L, et al.; AACE/AME/ETA Task Force on Thyroid Nodules. American Association of Clinical Endocrinologists, Associazione Medici Endocrinologi, and EuropeanThyroid Association medical guidelines for clinical practice for the diagnosis and management of thyroid nodules. *Endocr Pract* 2010;16 Suppl 1:1-43
14. Algin O, Algin E, Gokalp G, Ocakoğlu G, Erdoğan C, Saraydaroglu O, et al. Role of duplex power Doppler ultrasound in differentiation between malignant and benign thyroid nodules. *Korean J Radiol* 2010;11:594-602
15. Moon HJ, Kwak JY, Kim MJ, Son EJ, Kim EK. Can vascularity at power Doppler US help predict thyroid malignancy? *Radiology* 2010;255:260-269
16. Lacout A, Marcy PY. Highlights on power Doppler US of thyroid malignancy. *Radiology* 2010;257:586-587; author reply 587
17. Tamsel S, Demirpolat G, Erdogan M, Nart D, Karadeniz M, Uluer H, et al. Power Doppler US patterns of vascularity and spectral Doppler US parameters in predicting malignancy in thyroid nodules. *Clin Radiol* 2007;62:245-251
18. Ophir J, Alam SK, Garra B, Kallel F, Konofagou E, Krouskop T, et al. Elastography: ultrasonic estimation and imaging of the elastic properties of tissues. *Proc Inst Mech Eng H* 1999;213:203-233
19. Gao L, Parker KJ, Lerner RM, Levinson SF. Imaging of the elastic properties of tissue--a review. *Ultrasound Med Biol* 1996;22:959-977
20. Greenleaf JF, Fatemi M, Insana M. Selected methods for imaging elastic properties of biological tissues. *Annu Rev Biomed Eng* 2003;5:57-78
21. Garra BS, Cespedes EI, Ophir J, Spratt SR, Zuurbier RA, Magnant CM, et al. Elastography of breast lesions: initial clinical results. *Radiology* 1997;202:79-86
22. Stoian D, Cornianuz M, Dobrescu A, Lazăr F. Nodular thyroid cancer. Diagnostic value of real time elastography. *Chirurgia* (Bucur) 2012;107:39-46
23. Cosgrove D, Piscaglia F, Bamber J, Bojunga J, Correas JM, Gilja OH, et al. EFSUMB guidelines and recommendations on the clinical use of ultrasound elastography. Part 2: clinical applications. *Ultraschall Med* 2013;34:238-253
24. Bae U, Dighe M, Dubinsky T, Minoshima S, Shamdasani V, Kim Y. Ultrasound thyroid elastography using carotid artery pulsation: preliminary study. *J Ultrasound Med* 2007;26:797-805
25. Lyshchik A, Higashi T, Asato R, Tanaka S, Ito J, Mai JJ, et al. Thyroid gland tumor diagnosis at US elastography. *Radiology* 2005;237:202-211
26. Lim DJ, Luo S, Kim MH, Ko SH, Kim Y. Interobserver agreement and intraobserver reproducibility in thyroid ultrasound elastography. *AJR Am J Roentgenol* 2012;198:896-901
27. Cho YJ, Ha EJ, Han M, Choi JW. US elastography using carotid artery pulsation may increase the diagnostic accuracy for thyroid nodules with US-pathology discordance. *Ultrasound Med Biol* 2017;43:1587-1595
28. Youden WJ. Index for rating diagnostic tests. *Cancer* 1950;3:32-35
29. Dighe M, Bae U, Richardson ML, Dubinsky TJ, Minoshima S, Kim Y. Differential diagnosis of thyroid nodules with US elastography using carotid artery pulsation. *Radiology* 2008;248:662-669
30. Dighe M, Kim J, Luo S, Kim Y. Utility of the ultrasound elastographic systolic thyroid stiffness index in reducing fine-needle aspirations. *J Ultrasound Med* 2010;29:565-574
31. Dighe M, Luo S, Cuevas C, Kim Y. Efficacy of thyroid ultrasound elastography in differential diagnosis of small thyroid nodules. *Eur J Radiol* 2013;82:e274-e280
32. Cantisani V, Lodise P, Di Rocco G, Grazhdani H, Giannotti D, Patrizi G, et al. Diagnostic accuracy and interobserver agreement of quasistatic ultrasound elastography in the diagnosis of thyroid nodules. *Ultraschall Med* 2015;36:162-167
33. Choi WJ, Park JS, Koo HR, Kim SY, Chung MS, Tae K. Ultrasound elastography using carotid artery pulsation in the differential diagnosis of sonographically indeterminate thyroid nodules. *AJR Am J Roentgenol* 2015;204:396-401
34. Hong Y, Liu X, Li Z, Zhang X, Chen M, Luo Z. Real-time ultrasound elastography in the differential diagnosis of benign and malignant thyroid nodules. *J Ultrasound Med* 2009;28:861-867
35. Rago T, Santini F, Scutari M, Pinchera A, Vitti P. Elastography: new developments in ultrasound for predicting malignancy in thyroid nodules. *J Clin Endocrinol Metab* 2007;92:2917-2922
36. Baloch ZW, Tam D, Langer J, Mandel S, LiVolsi VA, Gupta PK. Ultrasound-guided fine-needle aspiration biopsy of the thyroid: role of on-site assessment and multiple cytologic preparations. *Diagn Cytopathol* 2000;23:425-429
37. Rago T, Di Coscio G, Basolo F, Scutari M, Elisei R, Berti P, et al. Combined clinical, thyroid ultrasound and cytological features help to predict thyroid malignancy in follicular and Hupsilonrthle cell thyroid lesions: results from a series of 505 consecutive patients. *Clin Endocrinol (Oxf)* 2007;66:13-20
38. Rhee SJ, Hahn SY, Ko ES, Ryu JW, Ko EY, Shin JH. Follicular variant of papillary thyroid carcinoma: distinct biologic behavior based on ultrasonographic features. *Thyroid* 2014;24:683-688
39. Kim MH, Luo S, Ko SH, Bae JS, Lim J, Lim DJ, et al. Thyroid nodule parameters influencing performance of ultrasound elastography using intrinsic compression. *Ultrasound Med Biol* 2015;41:2333-2339